arXiv:1609.03735v1 [physics.flu-dyn] 13 Sep 2016

Discrete Boltzmann model of shallow water equations with polynomial equilibria

Jianping Meng,* Xiao-Jun Gu,† and David R Emerson‡
Scientific Computing Department, STFC Daresbury laboratory, Warrington WA4 4AD, United Kingdom

Yong Peng§ and Jianmin Zhang¶
State Key Laboratory of Hydraulics and Mountain River Engineering, Sichuan University, Chengdu, 610065, P. R. China

A hierarchy of discrete Boltzmann model is proposed for simulating shallow water flows. By using the Hermite expansion and Gauss-Hermite quadrature, the conservation laws are automatically satisfied without extra effort. Moreover, the expansion order and quadrature can be chosen flexibly according to the problem for striking the balance of accuracy and efficiency. The models are then tested using the classical one-dimensional dam-breaking problem, and successes are found for both supercritical and subcritical flows.

I. INTRODUCTION

There is significant interest in modelling shallow water flows at the mesoscopic level, either utilising the mesoscopic information or directly simulating at the mesoscopic scale. For the first approach, the gas-kinetic scheme (GKS) was proposed [1, 2], in which a Boltzmann type equation with the **B**hatnagar-**G**ross-**K**rook (BGK) is used as an intermediate step to supplement the flux term of shallow water equations (SWEs) [1]. In the literature, the GKS has been applied for a range of flows including strong shock and dam-breaking problems [1, 3, 4]. For the second direction, the main approach is the lattice Boltzmann method (LBM). The LBM can be considered as a special case of discrete velocity method (DVM) for which a minimal discrete velocity set [5] is sought and tied to the discretisation in space [6]. In this way, the scheme is sufficiently simple yet powerful enough to handle complex flow problems. Hence, the scheme has also be extended to modelling of the SWEs[7–9].

A critical challenge for LBM is to simulate supercritical shallow water flows characterised by a high Froude (Fr) number. For this purpose, an asymmetric model is proposed in [10] for simulating one-dimensional flows with $Fr > 1$. In [11], a multi-speed scheme has been proposed recently by matching hydrodynamic moments and applied for both one-dimensional and two-dimensional supercritical flows. Since the discrete velocities are not integers in general, a finite difference scheme has to be used so that the scheme is best classified as a discrete Boltzmann model.

In this work, we have derived a hierarchy of **d**iscrete **B**oltzmann **m**odels with **p**olynomial **e**quilibria (DBMPE) from the continuous Boltzmann-BGK type equation using the Hermite expansion approach [12, 13]. From this framework, we can have both integer and non-integer discrete velocity sets, and then we are able to choose either particle-hoping like scheme or general finite difference scheme. The order of expansion may be easily tuned according to the requirement of the flow to be simulated.

II. DISCRETE BOLTZMANN MODEL

A. Derivation

If the depth scale is much less than the horizontal length scale, the water flows are dominated by the nearly horizontal motio and are referred as shallow water flows. For these flows, the SWEs can be employed to simplify the modelling, which are written as [14]

$$\frac{\partial h}{\partial t} + \boldsymbol{\nabla}\cdot(h\boldsymbol{V}) = 0 \tag{1}$$

and

$$\frac{D\boldsymbol{V}}{Dt} = -\frac{1}{h}\boldsymbol{\nabla}\mathcal{P} + \boldsymbol{F} + \boldsymbol{\nabla}\cdot\boldsymbol{\sigma}, \tag{2}$$

where

$$\boldsymbol{\sigma} = \nu h[\boldsymbol{\nabla}\boldsymbol{V} + (\boldsymbol{\nabla}\boldsymbol{V})^T - (\boldsymbol{\nabla}\cdot\boldsymbol{V})\boldsymbol{\delta}] \approx h\nu\triangle\boldsymbol{V},$$

and $\boldsymbol{\delta}$ (i.e., δ_{ij}) is the unit tensor. The equations describe the evolution of depth, h, and depth-averaged velocity, $\boldsymbol{V} = (u, v)$. The flows are often driven by a body force, $\boldsymbol{F}$, which mathematically represents not only the effects of an actual body force, including geostrophic force and tide-raising forces, but also those of wind stress, surface slope and atmospheric pressure gradient. The pressure

$$\mathcal{P} = \frac{hgh}{2} \tag{3}$$

* Corresponding author. jianping.meng@stfc.ac.uk;
Jianping Meng and Yong Peng contributed equally to this work and should be considered as co-first authors.
† xiaojun.gu@stfc.ac.uk
‡ david.emerson@stfc.ac.uk
§ pengyongscu@foxmail.com
¶ zhangjianmin@scu.edu.cn

originates from the hydrostatic assumption, where g represents for the gravitational force. If necessary, the viscous term $h\nu\triangle \boldsymbol{V}$ may also be considered where ν is the depth averaged kinetic viscosity. As has been shown, the SWEs can be mathematically analogous to the 2D compressible flow equations. In fact, it may be considered to be describing an ideal gas flow with a gas state equation Eq. (3), and its ratio of specific heats is $\gamma = 2$ and the "sound speed" is $\sqrt{gh}$ (cf. Chapter 2.1 in [14]).

A Boltzmann-BGK type equation can then be constructed for SWEs [1],

$$\frac{\partial f}{\partial t} + \boldsymbol{c}\cdot\frac{\partial f}{\partial \boldsymbol{r}} + \boldsymbol{F}\cdot\frac{\partial f}{\partial \boldsymbol{c}} = \frac{f^{eq}-f}{\tau} \tag{4}$$

where

$$f^{eq} = \frac{1}{\pi g}\exp[\frac{(\boldsymbol{c}-\boldsymbol{V})\cdot(\boldsymbol{c}-\boldsymbol{V})}{gh}]. \tag{5}$$

At the mesoscopic scale, the evolutionary variable becomes the distribution function $f(\boldsymbol{r},\boldsymbol{c},t)$ which represents the number of particles in the volume $d\boldsymbol{r}$ centred at position $\boldsymbol{r}=(x,y)$ with velocities within $d\boldsymbol{c}$ around velocity $\boldsymbol{c}=(c_x,c_y)$ at time t. The macroscopic quantities can be obtained by integrating over the whole particle velocity space, i.e.,

$$h = \int f d\boldsymbol{c} = \int f^{eq} d\boldsymbol{c}, \tag{6}$$

$$h\boldsymbol{V} = \int f\boldsymbol{c} d\boldsymbol{c} = \int f^{\boldsymbol{eq}}\boldsymbol{c} d\boldsymbol{c}, \tag{7}$$

and

$$2\mathcal{P} = hgh = \int f(\boldsymbol{c}-\boldsymbol{V})\cdot(\boldsymbol{c}-\boldsymbol{V})d\boldsymbol{c}. \tag{8}$$

Moreover, the **r**ight-**h**and **s**ide (RHS) term of Eq. (4) obeys the conservation property of the collision integral as shown in Eqs. (6) and (7). Similar to a real ideal gas, the relation between the relaxation time and kinetic viscosity is

$$\nu h = \mathcal{P}\tau, \tag{9}$$

which can be obtained by using the Chapman-Enskog expansion.

In principle, this kinetic equation may be solved directly by using regular numerical discretisation for both physical and particle velocity, i.e., the so-called discrete velocity method. Compared with direct discretisation of SWEs, there are two more degrees of freedom for the particle velocity, which need to be treated carefully for both accuracy and efficiency. Among various schemes, the Gauss type quadrature can provide a very efficient yet simple to implement discretisation if properly truncating the equilibrium function Eq. (5). We shall derive a hierarchy of discrete Boltzmann models using a Hermite expansion [12, 13]. However, it is convenient to first introduce a non-dimensional system,

$$\hat{\boldsymbol{r}} = \frac{\boldsymbol{r}}{h_0}, \hat{\boldsymbol{V}} = \frac{\sqrt{2}\boldsymbol{V}}{\sqrt{gh_0}}, \hat{t} = \frac{\sqrt{gh_0}t}{\sqrt{2}h_0}, \hat{\boldsymbol{F}} = 2\frac{\boldsymbol{F}}{g}, \tag{10}$$

$$\hat{\boldsymbol{c}} = \frac{\sqrt{2}c}{\sqrt{gh_0}}, \hat{f} = f\frac{g}{2}, \hat{\nu} = \frac{\nu}{\nu_0}, \hat{h} = \frac{h}{h_0}, \hat{\mathcal{P}} = \frac{\mathcal{P}}{\mathcal{P}_0} = \hat{h}^2,$$

where the hat symbol denotes the non-dimensional variables. The reference depth, h_0, can be the characteristic depth of the system such as the depth at the inlet (e.g., h_l in Fig. 2), while the reference viscosity is represented by ν_0 and the reference pressure $\mathcal{P}_0$ is chosen as $gh_0^2/2$. By using these non-dimensional variables, Eqs. (4) and (5) become,

$$\frac{\partial \hat{f}}{\partial \hat{t}} + \hat{\boldsymbol{c}}\cdot\frac{\partial \hat{f}}{\partial \hat{\boldsymbol{r}}} + \hat{\boldsymbol{F}}\cdot\frac{\partial \hat{f}}{\partial \hat{\boldsymbol{c}}} = \frac{\mathcal{P}_0}{\nu_0\sqrt{gh_0/2}}\frac{\hat{\mathcal{P}}}{\hat{\nu}\hat{h}}(\hat{f}^{eq}-\hat{f}), \tag{11}$$

and

$$\hat{f}^{eq} = \frac{1}{2\pi}\exp[\frac{(\hat{\boldsymbol{c}}-\hat{\boldsymbol{V}})\cdot(\hat{\boldsymbol{c}}-\hat{\boldsymbol{V}})}{2\hat{h}}], \tag{12}$$

while there is no need to change the form of Eqs. (6) -(8). We may also define a "Knudsen" number

$$\mathcal{K} = \frac{\nu_0\sqrt{gh_0/2}}{\mathcal{P}_0} = \frac{\nu_0\sqrt{gh_0/2}}{gh_0^2/2}, \tag{13}$$

and the local Froude number becomes

$$Fr = \frac{U}{\sqrt{gh}} = \frac{\hat{U}\sqrt{gh_0/2}}{\sqrt{g\hat{h}h_0}} = \frac{\hat{U}}{\sqrt{2\hat{h}}}, \tag{14}$$

where the velocity magnitude is denoted by U. Using the "Knudsen" number and considering the fact that the viscosity is often considered as constant, the RHS term of Eq.(11) becomes,

$$\frac{\hat{h}}{\mathcal{K}}(\hat{f}^{eq}-\hat{f}).$$

Hence, the actual relaxation time will change with time locally. Hereinafter, we shall use the non-dimensional version of quantities and equations by default, and the hat symbol will be omitted for clarity. It is also convenient to use the symbol τ to substitute for $\mathcal{K}/\hat{h}$ in writing the equations.

First of all, the equilibrium distribution will be expanded on the basis of the Hermite orthogonal polynomials$\boldsymbol{\chi}^{(n)}(\boldsymbol{c})$ in particle velocity space (see Ref. [12] for detail), i.e.,

$$f^{eq} \approx f^N_{eq} = \omega(\boldsymbol{c}) \sum_{n=0}^{N} \frac{1}{n!} \boldsymbol{a}^{(n)}_{eq} : \boldsymbol{\chi}^{(n)}(\boldsymbol{c}), \tag{15}$$

where the N^{th} order terms are retained and the coefficient is given yb

$$\boldsymbol{a}^{(n)}_{eq} = \int f^{eq} \boldsymbol{\chi}^{(n)} d\boldsymbol{c} \approx \sum_{\alpha=1}^{d} \frac{w_\alpha}{\omega(\boldsymbol{c}_\alpha)} f^N_{eq} \boldsymbol{\chi}^n(\boldsymbol{c}_\alpha). \tag{16}$$

Using Gauss-Hermite quadrature with weights w_α and abscissae $\boldsymbol{c}_\alpha$, $\alpha = 1, \cdots, d$, the integration in Eq. (16) has been converted into a summation. The first few coefficients are given by

$$a^{(0)}_{eq} = h, \tag{17}$$

$$\boldsymbol{a}^{(1)}_{eq} = h\boldsymbol{V}, \tag{18}$$

$$\boldsymbol{a}^{(2)}_{eq} = h[\boldsymbol{V}^2 + (h-1)\boldsymbol{\delta}], \tag{19}$$

$$\boldsymbol{a}^{(3)}_{eq} = h[\boldsymbol{V}^3 + (h-1)\boldsymbol{\delta V}], \tag{20}$$

and

$$\boldsymbol{a}^{(4)}_{eq} = h[\boldsymbol{V}^4 + (h-1)\boldsymbol{\delta V}^2 + (h-1)^2\boldsymbol{\delta}^2], \tag{21}$$

where tensor products such as $\boldsymbol{\delta V}$ stands for $V_i\delta_{jk} + V_j\delta_{ik} + V_k\delta_{ij}$. It is easy to verify that, with an appropriate quadrature, the conservation property of the collision integral will be satisfied automatically using an expansion higher than the first order, which will simplify the algorithm. The body force term $\mathcal{F}(\boldsymbol{x}, \boldsymbol{c}, t) = -\boldsymbol{F} \cdot \nabla_c f$ can also be approximated as,

$$\mathcal{F}(\boldsymbol{x}, \boldsymbol{c}, t) = \omega(\boldsymbol{c}) \sum_{n=1}^{N} \frac{1}{(n-1)!} \boldsymbol{F}\boldsymbol{a}^{(n-1)} : \boldsymbol{\chi}^{(n)}, \tag{22}$$

where $\boldsymbol{a}^{(n)}$ is the corresponding coefficients for the distribution function, f. The first two are same the a^0_{eq} and $\boldsymbol{a}^{(1)}_{eq}$ while the higher order terms can be related to stress and heat flux. Through the expansion, the kinetic equation (11) can be rewritten in its truncated form, i.e.,

$$\frac{\partial f}{\partial t} + \boldsymbol{c} \cdot \frac{\partial f}{\partial \boldsymbol{r}} = -\frac{1}{\tau}(f - f^N_{eq}) + \mathcal{F}. \tag{23}$$

Thus, we will be solving an approximation of the original kinetic equation.

The second step is to discretise Eq. (23) in particle velocity space. The Gauss-Hermite quadrature is the natural choice. In one dimension, the discrete velocities c_α are just the roots of the Hermite polynomials, and the corresponding weights are determined by:

$$w_\alpha = \frac{n!}{[n\chi^{n-1}(c_\alpha)]^2}. \tag{24}$$

Given one-dimensional velocity sets, those of a higher-dimension can be constructed using the "production" formulae [12]. Once the discrete velocity set is chosen, the governing equation is discretised as

$$\frac{\partial f_\alpha}{\partial t} + \boldsymbol{c}_\alpha \cdot \frac{\partial f_\alpha}{\partial \boldsymbol{r}} = -\frac{1}{\tau}(f_\alpha - f^{eq}_\alpha) + \mathcal{F}_\alpha, \tag{25}$$

where $f_\alpha = w_\alpha f(\boldsymbol{r}, \boldsymbol{c}_\alpha, t)/\omega(\boldsymbol{c}_\alpha)$, $f^{eq}_\alpha = w_\alpha f^{eq}(\boldsymbol{r}, \boldsymbol{c}_\alpha, t)/\omega(\boldsymbol{c}_\alpha)$ and $\mathcal{F}_\alpha = w_\alpha \mathcal{F}(\boldsymbol{r}, \boldsymbol{c}_\alpha, t)/\omega(\boldsymbol{c}_\alpha)$. According to Eqs. (17) - (21) and (15), the explicit form of the fourth order, f^{eq}_α, is

$$\begin{aligned} f^{eq}_\alpha = h w_\alpha \{ & 1 \\ & + c_i V_i + \frac{1}{2}\left[(c_iV_i)^2 - V_iV_i + (h-1)(c_ic_i - 2)\right] \\ & + \underline{\frac{c_iV_i}{6}[(c_iV_i)^2 - 3V_iV_i + 3(h-1)(c_ic_i - 4)]} \\ & + \underline{\underline{\frac{1}{24}[(c_iV_i)^4 - 6(V_ic_i)^2V_jV_j + 3(V_jV_j)^2]}} \\ & + \underline{\underline{\frac{h-1}{4}[(c_ic_i - 4)((V_ic_i)^2 - V_iV_i) - 2(V_ic_i)^2]}} \\ & + \underline{\underline{\frac{(h-1)^2}{8}\left[(c_ic_i)^2 - 8c_ic_i + 8)\right]}} \\ \}, & \end{aligned} \tag{26}$$

where the underlined terms are of third order, those double underlined are of fourth order, and the others consist of the zero order, the first order and the second order terms.

We have already constructed a kind of DBMPE. In order to conduct a numerical simulation, the physical space $\boldsymbol{r}$ and the time t are yet to be discretised. For this purpose, any available scheme may be utilised according to the property of flow, such as an upwind scheme for space discretisation. In particular, if using abscissae consisting of integers, the lattice Boltzmann scheme

$$\begin{aligned} & \tilde{f}_\alpha(\boldsymbol{r} + \boldsymbol{c}_\alpha dt, t + dt) - \tilde{f}_\alpha(\boldsymbol{r}, t) = \\ & -\frac{dt}{\tau + 0.5dt}\left[\tilde{f}_\alpha(\boldsymbol{r}, t) - f^{eq}_\alpha(\boldsymbol{r}, t)\right] + \frac{\tau \mathcal{F}_\alpha dt}{\tau + 0.5dt} \end{aligned} \tag{27}$$

can be constructed by introducing

$$\tilde{f}_\alpha = f_\alpha + \frac{dt}{2\tau}(f_\alpha - f^{eq}_\alpha) - \frac{dt}{2}F_\alpha,$$

which allows a kind of particle-hopping like feature. Due to this unique property, the lattice Boltzmann method has attracted significant interests in broad areas including shallow water simulations. However, if a high-order expansion is used, the abscissae will not be integer in general so that more sophisticated schemes will be required to solve the DBMPE. For instance, we will use an implicit-explicit (IMEX) scheme below for testing.

B. Remarks on accuracy

We are now ready to discuss a few aspects on the accuracy of DBMPE. As previously shown, errors are introduced in truncating the equilibrium function and discretising the particle velocity, i.e., from Eq. (11) to Eq. (23) and from Eq. (23) to Eq. (25).

In principle, if the order of the Hermite expansion is sufficiently high, Eq. (23) is expected to accurately recovery Eq. (11). In practice, however, only a few orders may be affordable in term of computational cost, and the approximation accuracy will be determined by the expansion order. In general, the accuracy will be related to the Froude number, i.e., higher Froude numbers may need more expansion terms, cf. Eq. (12) and Eq. (14). For instance, similar to gas dynamics, see Ref. [15], using a first-order expansion leads to a linear equation which is suitable when $Fr \to 0$. Specifically, we may introduce a L^2 norm

$$E_T = \sqrt{\frac{\int (f^{eq} - f^N_{eq})^2 d\boldsymbol{c}}{\int (f^{eq})^2 d\boldsymbol{c}}}$$

to measure the displacement of f^N_{eq} from f^{eq} over the whole particle velocity space. In Fig. 1, the density plots of E_T are shown over the macroscopic velocity range of $u \in \{-2, 2\}$ and $v \in \{-2, 2\}$. For comparison, we consider both the second-order expansion and fourth-order expansion of the equilibrium distribution function. From the plots, we clearly see that the error grows with increasing macroscopic velocities. In particular, with a smaller h, the error may become relatively large (note that E_T represents an accumulation of errors from all discrete velocities) with relatively small macroscopic velocities. Hence, simulations may be more prone to error and instability if there is a sharp horizontal gradient of depth which often induces fast water flow. Interestingly, it appears that a high-order expansion does not necessarily means smaller errors (see the plots for $h = 0.001$). This shows complex convergence behaviour of the Hermite expansion. However, since the conservation laws are retained naturally, even with limited expansion order, the DBMPE may be sufficient for a broad range of the hydrodynamic problems, particularly if the diffusion term plays a negligible role.

The second kind of error is from the chosen quadrature. According to the Chapman-Enskog expansion, when the "Knudsen" number $\mathcal{K}$ is small, the first-order asymptotic solution of Eq. (23) may be written as

$$f^{(1)} = -\tau(\partial_t^{(0)} + \boldsymbol{c} \cdot \boldsymbol{\nabla} + \boldsymbol{F} \cdot \boldsymbol{\nabla}_c) f^{(0)}, \tag{28}$$

where the zeroth-order solution, $f^{(0)}$, is just the truncated equilibrium function, f^N_{eq}. From Eq. (28), $f^{(1)}$ will include a polynomial of $\boldsymbol{c}$ of one order higher than that in $f^{(0)}$. Therefore, to numerically evaluate the integration of Eqs. (6) to (8), we need a quadrature with the degree of precision

$$P = 2d - 1 \geq N + 1 + M,$$

to calculate the M^{th} order of moment (e.g., $M = 0$ for the zeroth-order moment, h). Specifically, if using a 4^{th} order Hermite expansion and to get the stress right ($M = 2$), we need at least a quadrature with the 7^{th} order of precision, which may need four discrete velocities.

III. NUMERICAL VALIDATION

In the following, we test the scheme by simulating the transient evolution of an initial discontinuity of water level, i.e., the classical 1D dam-breaking problem. By utilising Eq. (15), the Hemite abscissae and Eq. (24), it is straightforward to construct various discrete velocity sets. For instance, to capture the strong shock with high Froude number, we may need to use a fourth order expansion for f^{eq}_α and a quadrature of at least 7^{th} order of precision. In contrast, if the flow is subcritical, then it may be enough to employ commonly used abscissae of nine points and a second order expansion for f^{eq}_α. We will test both scenarios. When the fourth expansion terms are employed for f^{eq}_α, we use a set of 16 discrete velocities obtained from the roots of fourth order Hermite polynomial, see Eq. (24). These 16 discrete velocities are not integer and require a finite difference scheme. For this purpose, we employ an IMEX scheme [16], which is particularly suitable if an solution is pursued at the Euler-limit when τ is typically small, i.e.,

$$f^{n+1}_\alpha = \frac{\tau^{n+1}}{\Upsilon}(f^n_\alpha - dt\boldsymbol{c}\cdot\boldsymbol{\nabla} f^n_\alpha) + \frac{dt}{\Upsilon} f^{eq}_\alpha(h^{n+1}, \boldsymbol{V}^{n+1}) \tag{29}$$

where

$$(h^{n+1}, \boldsymbol{V}^{n+1}) = \int (1, \boldsymbol{c})(f^n - dt\boldsymbol{c}\cdot\boldsymbol{\nabla} f^n_\alpha) d\boldsymbol{c}, \tag{30}$$

and

$$\Upsilon = \tau^{n+1} + dt.$$

The force term is ignored here since it is not involved in the test case. To cope with the strong discontinuity, the flux term is discretised as (cf. Ref. [17])

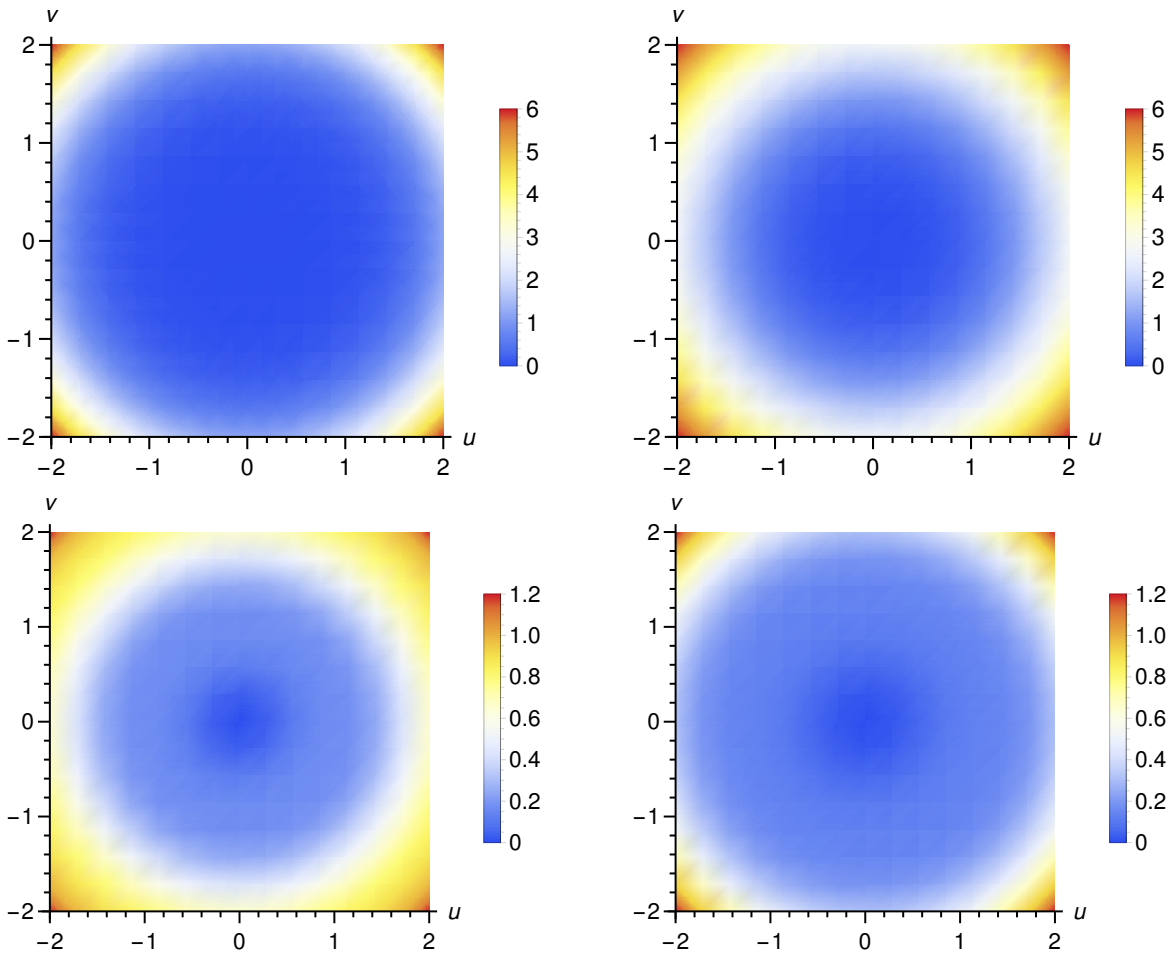

Figure 1. Profiles of E_T with coloured value when the second-order (left) and fourth-order (right) expansion are used repectively for f_{eq}^N at $h = 1$ (top) and $h = 0.001$ (bottom) .

$$c_x \frac{\partial f_\alpha}{\partial x} = \zeta(f_{\alpha,i} - f_{\alpha,I-1}) - \frac{1}{2}\zeta dx[sgn(\zeta) - \zeta](\sigma_{\alpha,i} - \sigma_{\alpha,I-1}) \tag{31}$$

where

$$\sigma_{\alpha,i} = \frac{f_{\alpha,i+1} - f_{\alpha,i-1}}{dx}\phi_{\alpha,i}(\theta_{\alpha,i})$$

and the van Leer slope limiter

$$\phi_{\alpha,i}(\theta_{\alpha,i}) = \frac{\theta_{\alpha,i} + |\theta_{\alpha,i}|}{\theta_{\alpha,i} + 1} \quad \theta_{\alpha,i} = \frac{f_{\alpha,i} - f_{\alpha,i-1}}{f_{\alpha,i+1} - f_{\alpha,i}}$$

For simplicity, only the discretisation in the x direction is given here. The choice of the subscript I in Eq. (31) also depends on the the sign c_x. If $c_x < 0$ ($c_x > 0$) the information is acquired from the grid point $I = i + 1$ ($I = i$). The mesh size is denoted by dx and $\zeta = c_x/dx$.

In simulations, we set the whole domain length to be 1000 in the non-dimensional system (i.e., $1000h_l$ in the dimensional system since the initial depth h_l at the inlet is chosen as the reference length). An initial discontinuity will be put at the middle $x = 500$ (see Fig. 2). For supercritical flow, the initial water depth is $h_l = 1$ at the left half domain (i.e., the reference length scale) and $h_r = 0.001$ at the right half, while for the subcritical case, the ratio is $1 : 0.25$.

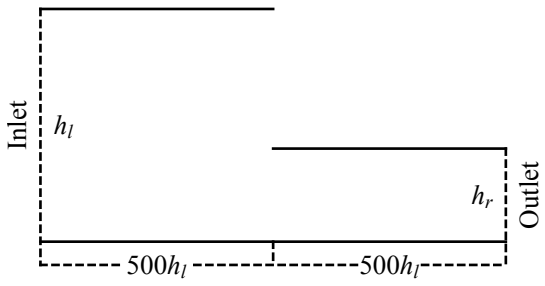

Figure 2. Illustration of the problem setup at the initial time.

For supercritical flow, the parameters for calculation

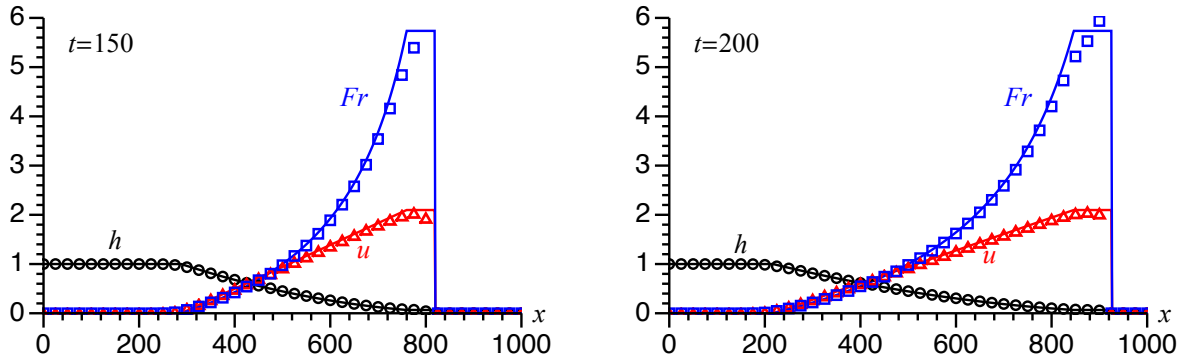

Figure 3. Profiles of depth, velocity and local Froude number for $h_l : h_r = 1000 : 1$. Lines and symbols represent analytical and numerical solutions, respectively.

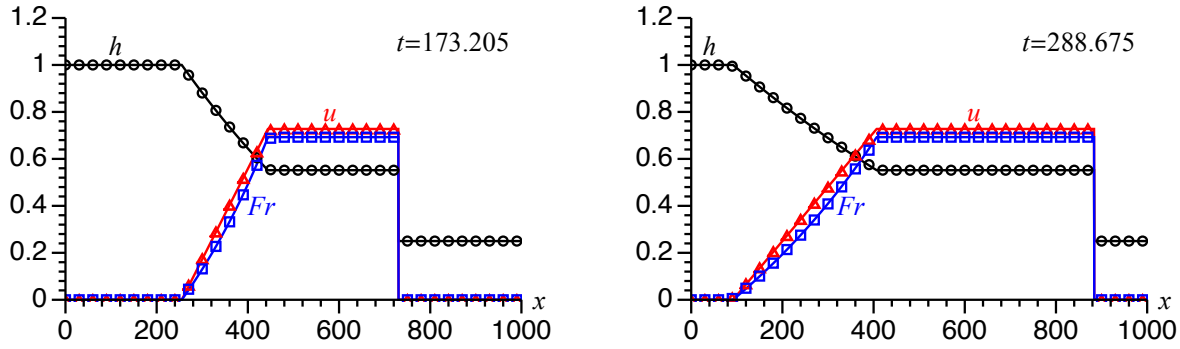

Figure 4. Profiles of depth, velocity and local Froude number for $h_l : h_r = 4 : 1$. Lines and symbols represent analytical and numerical solutions, respectively.

are chosen as

$$\mathcal{K} = 10^{-7}, dx = \frac{1}{600}, dt = 0.05.$$

The results at $t = 150$ and $t = 200$ are shown in Fig. 3. Excellent agreement is found for both water depth and velocity with the analytical solution (see Ref. [18] for details of theanalytical solution), although numerical error is found for the profile of local Froude number at the position of discontinuity due to the phase lag between water depth and velocity caused by numerical diffusion. The simulations confirms the capability of modelling supercritical flows with a fourth order expansion and corresponding quadrature. By contrast, we also tested the combination of a second-order expansion and 16 discrete velocities, but found that the simulation is unstable using the same problem setup.

For the subcritical flow, we use the stream-collision scheme (27) and the parameters are chosen as

$$\mathcal{K} = 0.1, dx = \frac{1}{2000}, dt = \frac{dx}{\sqrt{3}}.$$

While the stream-collision scheme is simpler, it requires a smaller time step for stable simulations due to the stiffness of the right hand collision term when $\mathcal{K}$ is small. Moreover, since the spatial mesh is tied to the time step, this requirement may cause quadratic increase of computational cost in 2D. The above parameters present an economic combination which results in very efficient simulations. The numerical results are shown in Fig. 4, where excellent agreement with the analytical solutions [18] can be found. Moreover, it appears that there is almost no numerical diffusion. However, possibly due to the low diffusion, the scheme limits the maximum local Froude number. Using the same expansion order and quadrature, the scheme (29) can simulate higher Froude number in general, in particular for supercritical flow.

IV. CONCLUDING REMARKS

To summarise, we have derived a hierarchy of discrete Boltzmann models with polynomial equilibria for modelling shallow water flows. Utilising the Hermite expansion and Gauss-Hermite quadrature, the scheme automatically satisfies the conservation property of the collision integral, which greatly simplifies the algorithm. We also discussed theoretically how to choose the expansion order and quadrature according the requirement of problems (e.g., Fr), although the Hermite expansion shows

complex convergence behaviour. In particular, if the quadrature consists of integer abscissae, we can obtain the very simple and efficient lattice Boltzmann scheme. The derived models are tested using the classical one-dimensional dam-breaking problem, excellent agreement with analytical solutions is found for both supercritical and subcritical flows. In the future, we will further investigate the application for more complicated problems, e.g., the treatment of force terms.

ACKNOWLEDGMENTS

Authors from Daresbury laboratory would like to thank the Engineering and Physical Science Research Council (EPSRC) for their support of Collaborative Computational Project 5 (CCP5) and UK Consortium on Mesoscale Engineering Sciences (UKCOMES, Grant No. EP/L00030X/1). Authors from Sichuan University would like to thank the support of the National Natural Science Foundation of China under grant numbers: 51409183, 51579166 and 5151101425.

[1] M. S. Ghidaoui, J. Q. Deng, W. G. Gray, and K. Xu, Int. J. Numer. Meth. Fl. **35**, 449 (2001).
[2] K. Xu, J. Comput. Phys. **178**, 533 (2002).
[3] J. H. Liang, M. S. Ghidaoui, J. Q. Deng, and W. G. Gray, J. Hydraul. Res. **45**, 147 (2007).
[4] P. Prestininzi, M. L. Rocca, A. Montessori, and G. Sciortino, Comput. Math. Appl. **68**, 439 (2014).
[5] Since a discrete velocity set is often from a quadrature for integration, we consider these two terminologies exchangeable here. In particular, if the discrete velocities are of integer numbers, the terminology "lattice" are also used.
[6] S. Chen and G. D. Doolen, Annu. Rev. Fluid Mech. **30**, 329 (1998).
[7] J. G. Zhou, Int. J. Mod. Phys. C **13**, 1135 (2002).
[8] J. G. Zhou, Comput. Method. Appl. M. **191**, 3527 (2002).
[9] J. G. Zhou, *Lattice Boltzmann methods for shallow water flows* (Springer, Berlin, 2004).
[10] B. Chopard, V. Pham, and L. Lefèvre, Comput. Fluids **88**, 225 (2013).
[11] M. L. Rocca, A. Montessori, P. Prestininzi, and S. Succi, J. Comput. Phys. **284**, 117 (2015).
[12] X. W. Shan, X. F. Yuan, and H. D. Chen, J. Fluid Mech. **550**, 413 (2006).
[13] X. Shan and X. He, Phys. Rev. Lett. **80**, 65 (1998).
[14] W. Y. Tan, *Shallow water hydrodynamics : mathematical theory and numerical solution for a two-dimensional system of shallow water equations* (Water & Power Press, China and Elsevier, Amsterdam, 1992).
[15] J. Meng and Y. Zhang, J. Comput. Phys. **230**, 835 (2011)
[16] F. Filbet and S. Jin, J. Sci. Comput. **46**, 204 (2011).
[17] S. Jin and Q. Li, Numer. Meth. Part. D. E. **29**, 1056 (2013).
[18] O. Delestre, C. Lucas, P.-A. Ksinant, F. Darboux, C. Laguerre, T. N. T. Vo, F. James, and S. Cordier, Int. J. Numer. Meth. Fl. **72**, 269 (2013).